microamorphous, and microaphanitic, and further on a geometric basis into microgranular, microlamellar, and microfibrous. More recently, Kloss[12] reported that, unlike macrocrystalline quartz crystals, microcrystalline quartz crystals generally show no sharp inversion point, and the inversion takes place over an interval of nearly 50° C. Our work suggests that it is best to describe the product of powdering quartz as microcrystalline quartz, which has an X-ray structure corresponding to quartz but is not normally detectable by d.t.a. unless carried out at high heating rates. In addition, this microcrystalline quartz contains chemisorbed H_2O.

We thank Professor R. A. Howie, Moreton Moore, E. Nave, N. Walsh and Miss P. S. Osborn, and the Science Research Council.

G. S. M. Moore
H. E. Rose

Powder Science Laboratory,
Department of Mechanical Engineering,
King's College, Strand,
London WC2

Received October 10, 1972.

[1] Dempster, P. B., and Ritchie, P. D., *J. Appl. Chem.*, **3**, 182 (1953).
[2] Hillebrand, W. F., *J. Amer. Chem. Soc.*, **30**, 1120 (1908).
[3] Keith, M. L., and Tuttle, O. F., *Amer. J. Sci.*, Bowen vol., 203 (1952).
[4] Ray, R. C., *Proc. Roy. Soc.*, **101**, A, 509 and 640 (1922).
[5] Sosman, R. B., and Merwin, H. E., *J. Wash. Acad. Sci.*, **14**, 117 (1924).
[6] Dale, A. J., *Trans. Brit. Ceram. Soc.*, **23**, 211 (1924).
[7] Clelland, D. W., and Ritchie, P. D., *J. Appl. Chem.*, **2**, 42 (1952).
[8] Dempster, P. B., and Ritchie, P. D., *J. Appl. Chem.*, **3**, 187 (1953).
[9] Sakabe, H., *et al.*, *Bull. Nat. Inst. Indust. Jap.*, **4**, 1 (1960).
[10] Soda, R., *J. Chem. Soc. Jap.*, **34**, 1491 (1961).
[11] Sosman, R. B., *The Phases of Silica*, 218 (Rutgers University Press, 1965).
[12] Smykatz-Kloss, W., *Contr. Mineral. Petrol.*, **36**, 1 (1972).

Image Formation by Induced Local Interactions: Examples Employing Nuclear Magnetic Resonance

An image of an object may be defined as a graphical representation of the spatial distribution of one or more of its properties. Image formation usually requires that the object interact with a matter or radiation field characterized by a wavelength comparable to or smaller than the smallest features to be distinguished, so that the region of interaction may be restricted and a resolved image generated.

This limitation on the wavelength of the field may be removed, and a new class of image generated, by taking advantage of induced local interactions. In the presence of a second field that restricts the interaction of the object with the first field to a limited region, the resolution becomes independent of wavelength, and is instead a function of the ratio of the normal width of the interaction to the shift produced by a gradient in the second field. Because the interaction may be regarded as a coupling of the two fields by the object, I propose that image formation by this technique be known as zeugmatography, from the Greek ζευγμα, "that which is used for joining".

The nature of the technique may be clarified by describing two simple examples. Nuclear magnetic resonance (NMR) zeugmatography was performed with 60 MHz (5 m) radiation and a static magnetic field gradient corresponding, for proton resonance, to about 700 Hz cm^{-1}. The test object consisted of two 1 mm inside diameter thin-walled glass capillaries of H_2O attached to the inside wall of a 4.2 mm inside diameter glass tube of D_2O. In the first experiment, both capillaries contained pure water. The proton resonance line width, in the absence of the transverse field gradient, was about 5 Hz. Assuming uniform signal strength across the region within the transmitter–receiver coil, the signal in the presence of a field gradient represents a one-dimensional projection of the H_2O content of the object, integrated over planes perpendicular to the gradient direction, as a function of the gradient coordinate (Fig. 1). One method of constructing a two-dimensional projected image of the object, as represented by its H_2O content, is to combine several projections, obtained by rotating the object about an axis perpendicular to the gradient direction (or, as in Fig. 1, rotating the gradient about the object), using one of the available methods for reconstruction of objects from their projections[1–5]. Fig. 2 was generated by an algorithm, similar to that of Gordon and Herman[4], applied to four projections, spaced as in Fig. 1, so as to construct a 20 × 20 image matrix. The representation shown was produced by shading within contours interpolated between the matrix points, and clearly reveals the locations and dimensions of the two columns of H_2O. In the second experiment, one capillary contained pure H_2O, and the other contained a 0.19 mM solution of $MnSO_4$ in H_2O. At low radio-frequency power (about 0.2 mgauss) the two capillaries gave nearly identical images in the

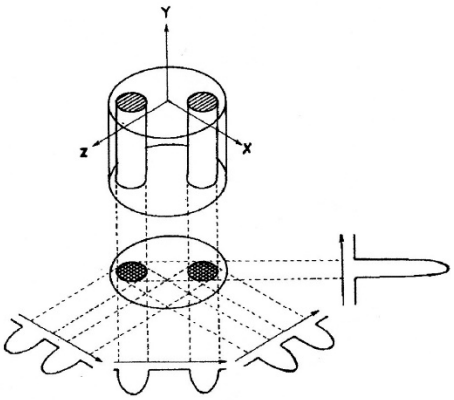

Fig. 1 Relationship between a three-dimensional object, its two-dimensional projection along the Y-axis, and four one-dimensional projections at 45° intervals in the XZ-plane. The arrows indicate the gradient directions.

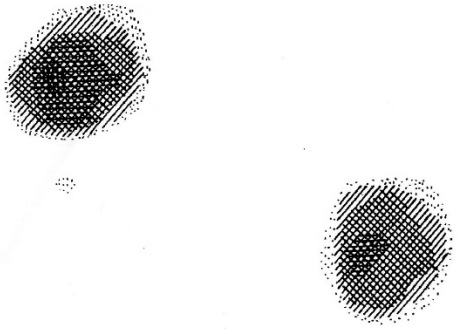

Fig. 2 Proton nuclear magnetic resonance zeugmatogram of the object described in the text, using four relative orientations of object and gradients as diagrammed in Fig. 1.

zeugmatogram (Fig. 3*a*). At a higher power level (about 1.6 mgauss), the pure water sample gave much more saturated signals than the sample whose spin-lattice relaxation time T_1 had been shortened by the addition of the paramagnetic Mn^{2+} ions, and its zeugmatographic image vanished at the contour level used in Fig. 3*b*. The sample region with long T_1 may be selectively emphasized (Fig. 3*c*) by constructing a difference zeugmatogram from those taken at different radio-frequency powers.

Applications of this technique to the study of various inhomogeneous objects, not necessarily restricted in size to those commonly studied by magnetic resonance spectroscopy, may be anticipated. The experiments outlined above demonstrate the ability of the technique to generate pictures of the distributions of stable isotopes, such as H and D, within an object. In the second experiment, relative intensities in an image were made to depend upon relative nuclear relaxation times. The variations in water contents and proton relaxation times among biological tissues should permit the generation, with field gradients large compared to internal magnetic inhomogeneities, of useful zeugmatographic images from the rather sharp water resonances of organisms, selectively picturing the various soft structures and tissues. A possible application of considerable interest at this time would be to the *in vivo* study of malignant tumours, which have been shown to give proton nuclear magnetic resonance signals with much longer water spin-lattice relaxation times than those in the corresponding normal tissues[6].

The basic zeugmatographic principle may be employed in many different ways, using a scanning technique, as described above, or transient methods. Variations on the experiment, to be described later, permit the generation of two- or three-dimensional images displaying chemical compositions, diffusion coefficients and other properties of objects measurable by spectroscopic techniques. Although applications employing nuclear magnetic resonance in liquid or liquid-like systems are simple and attractive because of the ease with which field gradients large enough to shift the narrow resonances by many line widths may be generated, NMR zeugmatography of solids, electron spin resonance zeugmatography, and analogous experiments in other regions of the spectrum should also be possible. Zeugmatographic techniques should find many useful applications in studies of the internal structures, states, and compositions of microscopic objects.

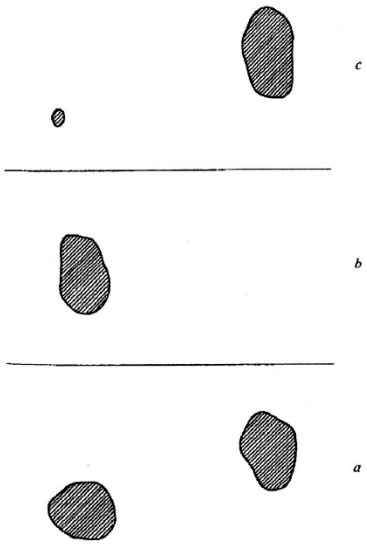

Fig. 3 Proton nuclear magnetic resonance zeugmatograms of an object containing regions with different relaxation times. *a*, Low power; *b*, high power; *c*, difference between *a* and *b*.

P. C. LAUTERBUR

Department of Chemistry,
State University of New York at Stony Brook,
Stony Brook, New York 11790

Received October 30, 1972; revised January 8, 1973.

1 Bracewell, R. N., and Riddle, A. C., *Astrophys. J.*, **150**, 427 (1967).
2 Vainshtein, B. K., *Soviet Physics–Crystallography*, **15**, 781 (1971).
3 Ramachandran, G. N., and Lakshminarayan, A. V., *Proc. US Nat. Acad. Sci.*, **68**, 2236 (1971).
4 Gordon, R., and Herman, G. T., *Comm. Assoc. Comput. Mach.*, **14**, 759 (1971).
5 Klug, A., and Crowther, R. A., *Nature*, **238**, 435 (1972).
6 Weisman, I. D., Bennett, L. H., Maxwell, Sr., L. R., Woods, M. W., and Burk, D., *Science*, **178**, 1288 (1972).

BIOLOGICAL SCIENCES

Island Lizards: the Genetic-Phenetic Variation Correlation

NATURAL populations of many organisms are known to contain much more genetic variation than would have been predicted by all but a minority[1] of geneticists two decades ago. Individuals of several species have up to 22% of their loci heterozygous, and from 0–50% or more of the loci in a population are polymorphic, although the higher estimates may result from sampling error[2–4]; vertebrates tend to be at the lower end of these ranges. Estimates such as these are based on electrophoretically detectable variation in proteins, so the true levels of genetic variation are probably higher[5]. These generalizations are gaining wide acceptance, but there is still some unease about their accuracy. The fundamental question is whether the loci being sampled are representative of the genome as a whole. We here present evidence that the electrophoretic approach is relatively unbiased.

Two groups of lizards were used: eight species of *Anolis* from the West Indies and thirteen populations of the side-blotched lizards *Uta stansburiana, sensu latu*, from California and Mexico, caught in 1971 and 1972. Geographic variation is not a source of heterogeneity, as all specimens from a locality were collected within a few hundred metres of one another. After capture, they were transported alive or on dry ice to the laboratory and stored at −76° C until needed. After skinning, water-soluble proteins were routinely extracted and electrophoresed[6]. Six of the eight *Anolis* species were from Puerto Rico, and two, *A. extremus* and *A. roquet*, were from Barbados and Martinique, respectively.

A single morphological character was used to estimate morphological variation in the *Anolis* species; the number of subdigital scales on the longest toe (second) on the hind foot, starting with the most distal lamella and counting proximally. Variability in this character is correlated with variability in other scale characters, but the other characters were not scored as accurately. Estimates of genetic variation in the *Anolis* species were derived from the starch-gel electrophoresis patterns of enzymes and nonenzymatic proteins, which together appear to represent the gene products of twenty-one or twenty-two loci. The proteins assayed were lactate dehydrogenases, malate dehydrogenases, α-glycerol-phosphate dehydrogenase, isocitrate dehydrogenases, indophenol oxidase, phosphoglucose isomerase, phosphoglutamase, glutamic oxaloacetate